



Structural and optical properties of GaN:Eu nanoparticles synthesized by simple ammonification method

Xiaojun Pan*, Xiuyun An, Zhenxing Zhang, Jinyuan Zhou, Erqing Xie

School of Physical Science and Technology, Lanzhou University, Lanzhou 730000, PR China

ARTICLE INFO

Article history:

Received 10 October 2011

Received in revised form 8 December 2011

Accepted 12 December 2011

Available online 8 January 2012

Keywords:

GaN:Eu nanoparticles

Photoluminescence

Ammonification method

ABSTRACT

GaN:Eu nanoparticles have been synthesized by simple ammonification of a mixture of $\text{Ga}(\text{NO}_3)_3$ and $\text{Eu}(\text{NO}_3)_3$. TEM images showed that the sizes of the particles were almost uniform, and the average grain sizes of the samples prepared at 850, 950, and 1050 °C were evaluated as 4.2 nm, 16.8 nm, and 24.3 nm, respectively. Except for conventional GaN Raman shifts, two extra peaks at 255 and 419 cm^{-1} observed in the Raman spectra could be attributed to the phonons activated by surface disorders or finite-size effects and vibration mode of N-rich octahedral Ga–N₆ bonds, respectively. From PL spectra, five characteristic peaks of Eu^{3+} ions were clearly observed: $^5\text{D}_1 \rightarrow ^7\text{F}_1$ (543 nm), $^5\text{D}_0 \rightarrow ^7\text{F}_1$ (592 nm), $^5\text{D}_0 \rightarrow ^7\text{F}_2$ (614 nm), $^5\text{D}_0 \rightarrow ^7\text{F}_3$ (652 nm), $^5\text{D}_0 \rightarrow ^7\text{F}_4$ (697 nm). Besides, the influences of the synthesized temperature and Eu^{3+} ion concentration on the PL behaviors were also studied.

© 2011 Elsevier B.V. All rights reserved.

1. Introduction

Gallium nitride (GaN) materials have been considered as promising materials for optoelectronic application such as ultraviolet–visible light emitting diodes (LEDs) and laser diodes (LDs), as well as high-temperature and high-power electronic devices, due to their direct wide band gaps, good thermal stability, and strongly emissive properties.

Rear earth (RE) doped semiconductors have been intensively and widely studied in recent years due to their prospective applications in many technological fields, such as photoelectric devices, solid state laser, flat plane displays, high energy radiation detectors [1]. From the point of view of band gap, GaN materials should also be considered as a promising candidate to be used for the host material of RE. As is expected, GaN:RE³⁺ materials can exhibit not only the photoelectronic properties of GaN material, but also the unique feature of luminescent properties of REs ions. Therefore, GaN:RE are attractive materials for studying the fundamental standpoint of structure composition properties of solids as well as applied perspectives.

During recent decades, the luminescence properties of GaN:REs films have been intensively investigated, indicating that this type of materials can emit from infrared to blue light region with high brightness, long life, good monochlor, and low quenching effect [1–9]. As well-known, quantum effects in intrinsic could result stronger emission and more efficient on doped nano-materials.

So far, the luminescent properties of GaN:RE powders have been studied by several groups. Podhorodecki et al. have reported luminescence and energy transfer process in GaN:Eu powder [10,11,25]. Brown et al. have prepared GaN:Eu powder by a Na Flux Method and obtained red emission [12]. In this paper, GaN:Eu nanoparticles have been synthesized by simple ammonification of Eu doped Ga_2O_3 . Ammonification method is a low cost and facile way to prepare GaN and doped GaN nanomaterials [13–16]. The optical properties of synthesized nanoparticles using Raman and PL were mainly studied. Besides, the influence of the synthesized conditions on PL was also discussed.

2. Experimental details

GaN:Eu nanoparticles have been synthesized by simple ammonification of Eu doped Ga_2O_3 . First, 2.5 g $\text{Ga}(\text{NO}_3)_3 \cdot x\text{H}_2\text{O}$ ($x = 7–9$, 99.99%) and 30 mg $\text{Eu}(\text{NO}_3)_3 \cdot 6\text{H}_2\text{O}$ (99.99%, about 1 at.%) were solubilized in 15 ml ethanol, followed by strong magnetic stirring for 30 min. Then, the mixture was put into an oven and dried at 60 °C for several hours. Second, the obtained dry powder was divided into three portions for ammonification at different temperatures. Three portions of powder were placed at three positions in an alumina crucible into quartz tube, and the powders were calcined at 850 °C, 950 °C, and 1050 °C in air to obtain Eu doped Ga_2O_3 . Finally, an ammonia (NH_3 , 99.85%) flow of 20 cm^3/min was introduced into the quartz tube for the in situ ammonification of the samples. The ammonification process was kept for 1 h at 950 °C. After nitridation, the furnace was cooled down to the room temperature under the NH_3 flowing to prevent oxidation.

Furthermore, in order to investigate the influence of the Eu^{3+} ion concentration on the luminescence intensities, different doping concentrations of Eu^{3+} ions (6, 30, 150 mg) were also tried out. To repeat the above process, both the calcinations and the ammonification temperatures were set to 950 °C.

After the samples preparation, X-ray diffraction (XRD) (Philips X'Pert Pro) with $\text{Cu K}\alpha$ ($\lambda = 0.154056$ nm) source was used to investigate the structure and grain size of the samples. The morphologies and microstructures were observed by transmission electron microscopy (TEM; JEOL JEM-2010F). Raman and Photoluminescence

* Corresponding author.

E-mail address: xjpan@lzu.edu.cn (X. Pan).

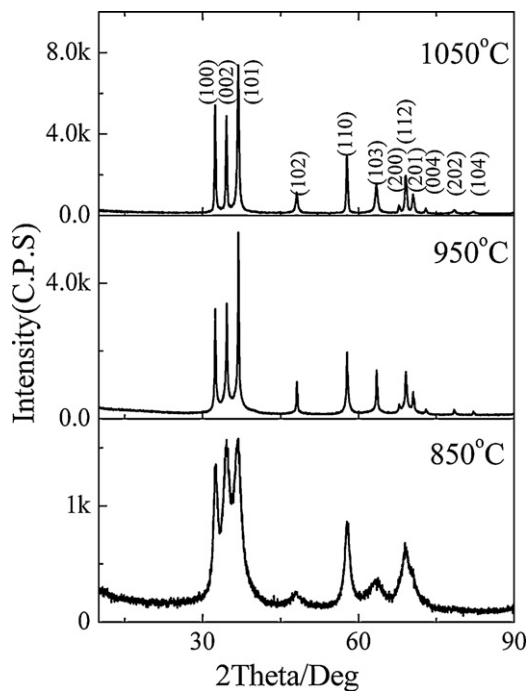


Fig. 1. XRD patterns of GaN:Eu (1 at.%) powders prepared at 850, 950 and 1050 °C, respectively.

(PL) spectra were recorded on a Jobin-Yvon LabRam HR80 spectrophotometer in backscattering geometry at room temperature, in which Raman spectra using 532 nm line of a 50 mW diode-pumped solid-state laser and PL spectra using 325 nm line of 35 mW He–Cd laser (Kimmon) as excitation sources. PL excitation (PLE) spectrum was recorded by a spectrophotometer (SHIMADZU RF-540).

3. Results and discussions

Fig. 1 shows XRD patterns of GaN:Eu powders prepared at 850, 950, and 1050 °C. All GaN:Eu powder samples predominantly exhibit hexagonal phase of GaN. For the samples prepared at 950 and 1050 °C, the most intense three peaks at $2\theta = 32.44^\circ$, 34.58° , and 36.85° correspond to (100), (002), and (101) planes of hexagonal GaN (h-GaN), respectively (JCPDF No. 02-1078). Moreover, the other lower peaks located at $2\theta = 48.14^\circ$, 57.77° , 63.46° , 67.74° , 69.18° , 70.52° , 72.92° , 78.37° , and 82.12° could correspond to (102), (110), (103), (200), (112), (201), (004), (202), and (104) planes of h-GaN phase, respectively. From XRD patterns, it can be found that the diffraction peaks of the powder prepared at 850 °C are much broader than the powders obtained at 950 and 1050 °C. This indicates that the crystallization of the samples increase as prepared temperature increasing.

In addition, the average crystal sizes of the powders can be usually calculated from the intense of (100), (002) and (101) diffraction peaks using the Scherrer formula [17]:

$$D(\text{nm}) = \frac{K\lambda}{(\beta_1^2 - \beta_0^2)^{1/2} \cos \theta}$$

where D is the crystal size; K is Scherrer constant with value of 0.89; λ is the wavelength of X-ray; β_1 is full width at half maximum (FWHM) of diffraction; β_0 is the peak broadening caused by the diffraction equipment; θ is the diffraction angle. There are some factors can contribute to the width of a diffraction peak, such as crystallite sizes, inhomogeneous strain, instrumental effects. In our condition, the crystallite sizes and instrumental effects are the main reasons. With high synthesized temperature and low doped concentration, the defects in nano-crystal could be ignored. The contribution of strain, which is very low resulted by defects, to

Table 1

The average sizes of GaN:Eu particles are estimated using most intense three peaks to be 4.2, 16.8, and 24.3 nm for 850, 950, and 1050 °C, respectively.

Ammonification temperature	FWHM ($^\circ$)			Average crystal size
	32.44 $^\circ$	34.58 $^\circ$	36.85 $^\circ$	
850 °C	1.433	2.116	2.428	4.2 nm
950 °C	0.202	0.238	0.167	16.8 nm
1050 °C	0.200	0.210	0.318	24.3 nm

width of peak in nanoparticles can be ignored. The values of instrumental broadening are 0.06° and 0.08° corresponding to $2\theta = 28.44^\circ$ and $2\theta = 55.73^\circ$ for standard Si sample, respectively. The average sizes of GaN:Eu particles are estimated using most intense three peaks to be 4.2, 16.8, and 24.3 nm for 850, 950, and 1050 °C, respectively, and shown in Table 1. The lattice constants of the sample prepared at 950 and 1050 °C can be calculated as $a = 3.2168 \text{ \AA}$, $c = 5.2315 \text{ \AA}$ and $a = 3.2198 \text{ \AA}$, $c = 5.2323 \text{ \AA}$, respectively, which are a little larger than the reference data ($a = 3.1891 \text{ \AA}$, $c = 5.1855 \text{ \AA}$) (JCPDS No. 50-0792). Eu atoms substitute Ga atoms in the crystal lattices causing distortion of lattice which results larger lattice constants after doped. XRD spectra show no diffraction lines of other phases.

For the further investigation the microstructure and morphologies of different ammonification temperature prepared powders (850, 950, and 1050 °C) were examined, TEM was used here and the results are shown in Fig. 2. The values of the particle sizes of GaN:Eu nanoparticles are consistent with those derived from XRD patterns.

Raman scattering is a very effect method to study properties of materials, it can provide lots of information of materials, such as optical, structure, carrier concentration properties, and so on. Raman scattering was also used here to investigate GaN:Eu powders. According to Orton and Foxon [20], h-GaN crystals or epilayers usually exhibit six first-order Raman active phonon modes in Raman spectra with peaks at 145 cm^{-1} ($E_2(\text{low})$), 533 ($A_1(\text{TO})$), 559 ($E_1(\text{TO})$), 569 ($E_2(\text{high})$), 735 ($A_1(\text{LO})$) and 743 ($E_1(\text{LO})$), respectively. In Fig. 3(a), on a broad background of the Raman spectrum, six peaks located at 255 , 331 , 419 , 535 , 569 , and 728 cm^{-1} can be observed. The peak at 728 cm^{-1} can be assigned to the $A_1(\text{LO})$ mode. The appearance of this mode might suggest that the carrier concentration of the powder samples is low [18].

The broad Raman scattering band of the sample synthesized at 1050 °C from 500 to 600 cm^{-1} can be fitted with three peaks using Lorentzian profiles, as shown in the inset of Fig. 4(a). These three peaks located at 528 , 558 and 568 cm^{-1} correspond to the $A_1(\text{TO})$, $E_1(\text{TO})$ and $E_2(\text{high})$ modes, respectively. Among all Raman shifts, the $E_2(\text{high})$ phonon peak is strongest, indicating that the samples possess a hexagonal crystal phase [19]. This is well consistent with the analysis derived from our XRD data. Additionally, the 331 cm^{-1} mode originates from the surface oxidation of Ga–O vibration [19].

The broadening behavior of the first-order Raman scattering modes of materials can be well demonstrated by spatial or phonon confinement models because that the phonons in nanosystems can usually be confined by crystallite boundaries or surface disorders [20–23]. In our previous research [24], similar broadening behaviors of the doped GaN nanostructures have been analyzed in details. Then, based on our previous research results, two extra Raman peaks at 255 and 419 cm^{-1} in this case can be attributed to the confinement by the C_{6v}^4 space group in first-order Raman scattering. The 255 cm^{-1} could be attributed to the phonons activated by surface disorders or finite-size effects [25]. According to Ning et al. [26], the vibrational mode of 418 cm^{-1} that frequently observed in GaN nanostructures can be caused by the octahedrally bonded structures of GaN. Thus, in view of the N-rich GaN nano-powder,

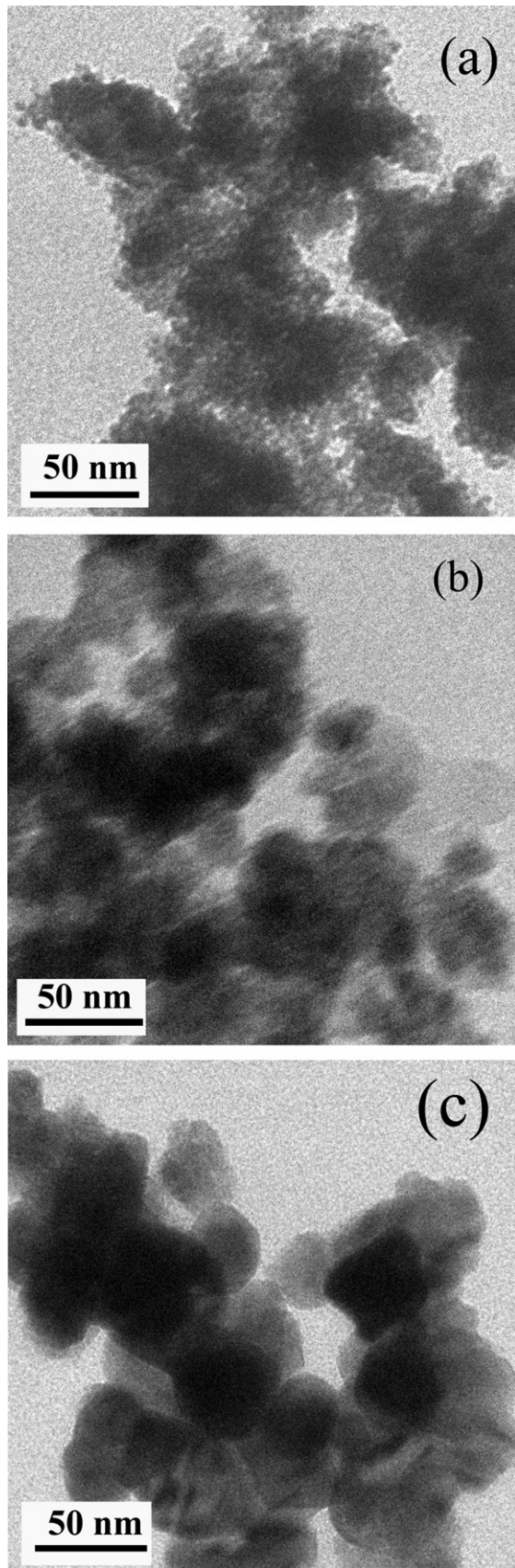


Fig. 2. TEM images of GaN:Eu nano-particles prepared at (a) 850 °C, (b) 950 °C, and (c) 1050 °C, respectively.

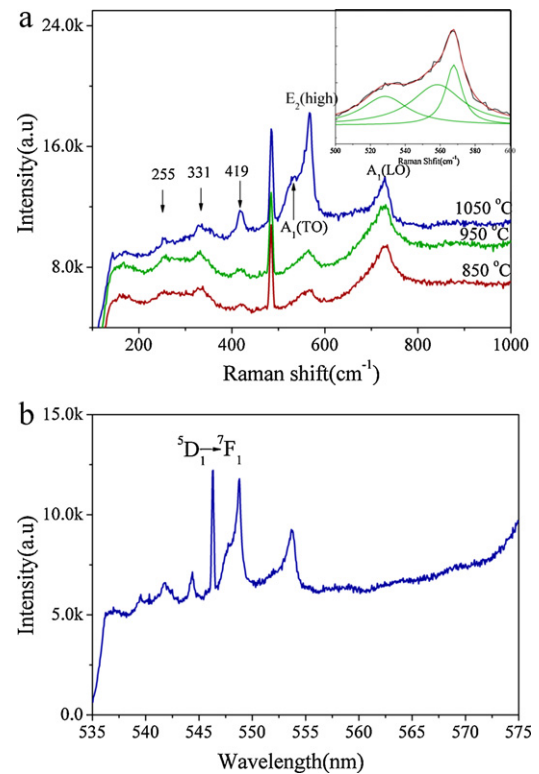


Fig. 3. (a) Room temperature Raman spectra of the GaN:Eu powder prepared at 850 °C, 950 °C, 1050 °C, excited by 532 nm laser. The inset shows the Raman shift between 500 and 600 cm^{-1} fitted with three peaks centered at 538, 558, 568 cm^{-1} using Lorentzian profile. (b) The nanometer coordinate unit of horizontal axis for the samples prepared at 1050 °C.

the 419 cm^{-1} Raman shift mode might be the vibration mode of N-rich octahedral Ga–N₆ bonds.

In Fig. 3(a), the Raman peak at 484 cm^{-1} is rather sharp-pointed, which can be assigned to intra-4*f* luminescence of Eu³⁺ ions [27]. In order to see it clearly, the coordinate unit (wavenumber (cm^{-1})) of horizontal axis was transformed into nanometer (nm), as shown Fig. 3(b). From the spectrum, the 484 cm^{-1} peak related with Eu³⁺ ions in Raman spectra using wavelength (nm) format is located at 546.2 nm (Raman spectra were excited by the 532 nm line of laser), which corresponds to the intra-4*f* $^5D_0 \rightarrow ^7F_1$ transition of Eu³⁺ ions.

Fig. 4 presents PL spectra of GaN:Eu powders at room temperature. Generally, h-GaN does not possess inversion symmetry but trigonal C_{3v} symmetry, which consequently relaxes the parity selection rule and leads to the strongest emission line at 615 nm of Eu³⁺ ion in all samples, as observed in Fig. 4. Such results suggest that Eu³⁺ ions are substituted for Ga atoms in crystal lattices. In all PL spectra, the four observed emission peaks correspond to the 4*f* → 4*f* intra-shell transitions of Eu³⁺ ions from the high excited states of 5D_1 or 5D_0 to the lower levels of 7F_J (*J* = 1, 3, 4): $^5D_1 \rightarrow ^7F_1$ (545 nm), $^5D_0 \rightarrow ^7F_1$ (598 nm), $^5D_0 \rightarrow ^7F_3$ (at 649 nm), $^5D_0 \rightarrow ^7F_4$ (at 682 nm), which prohibit electric-dipole and magnetic-dipole selection rules [27,28]. Besides, a broad emission band (G-band) in visible light region can also be observed in Fig. 4. According to Nyk et al. [29], the G-band is due to the lattice defects.

As mentioned above, the crystallinity of samples increased as the synthesis temperatures increasing. And, from Fig. 4(a), it can be seen that the intensities of PL spectra increase with the synthesized temperatures increasing. It can be concluded that increasing of PL intensity is closely related to the crystallinity of sample.

On the other hand, the PL intensities increase first and then reduce by raising the concentration of Eu³⁺ ions, as shown in Fig. 4(b). Such phenomenon would be explained as follows: the

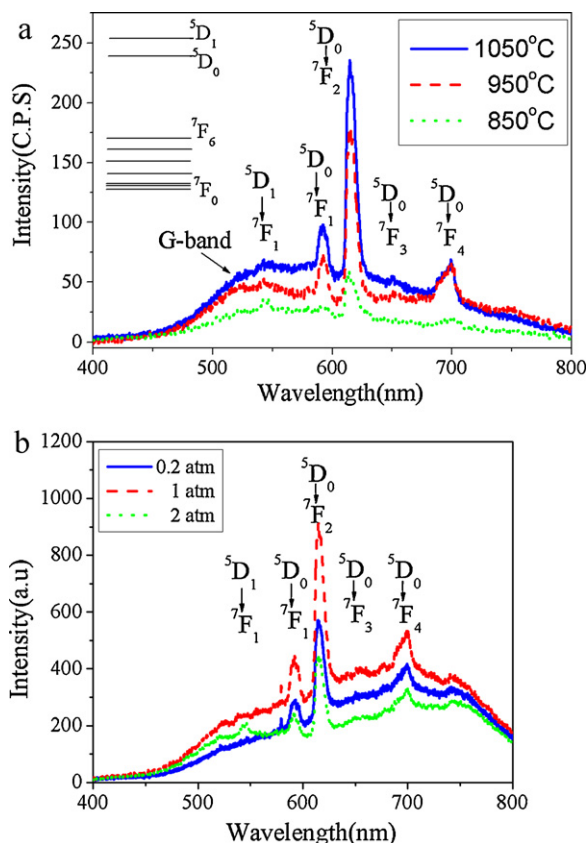


Fig. 4. (a) PL spectra of Eu-doped GaN powder prepared at 850, 950, 1050 °C. The inset shows Eu^{3+} ions related energy levels in the PL of GaN:Eu $^{3+}$ powder. (b) PL spectra of different Eu^{3+} concentration in GaN:Eu (0.2, 1, 5 atm) powder prepared at 950 °C.

number of effective luminous Eu^{3+} ions will increase under lower concentration with the increasing dopant concentration. Usually, the interaction of Eu^{3+} such as relaxation will also increase under higher RE concentration. As a result, the number of effective luminous Eu^{3+} ions decrease with further increasing the concentration of Eu^{3+} ions. Accordingly to PL spectra under high Eu^{3+} ion concentration, the emission of $5\text{D}_1 \rightarrow 7\text{F}_1$ (545 nm) appears, indicating that Eu^{3+} ions at 5D_1 level have no time relax to 5D_0 level. This is also direct evidence to confirm the above analysis.

In order to understand the energy transfer process between Eu^{3+} ions and GaN host matrix, PL excitation (PLE) spectrum was observed at 615 nm for Eu^{3+} -doped GaN nanoparticles prepared at 950 °C with Eu^{3+} ion concentration of 1%. As shown in Fig. 5, the strong excitation band ranging from 200 to 350 nm can be ascribed to the absorption of GaN host. There is another rather weaker peak at 482 nm is assigned to $7\text{F}_0 \rightarrow 5\text{D}_1$ transition in intra-4f shell of Eu^{3+} ion. Therefore, it can be concluded that the energy needing to excite the Eu^{3+} ions was mainly achieved from the direct band-gap absorption of GaN host matrix. After absorbed by the host matrix, the energy can be transferred to RE^{3+} ions by several routes. The RE ions substitute lattice positions of III atoms in III–V semiconductors could form isoelectronic impurities [30]. Due to electronegativity difference between III and RE atoms, the RE^{3+} ions could introduce electron/hole traps into III–V semiconductors and act as donors or acceptors. Such trap would be changed after attract either an electron or a hole. Then, the changed trap could capture an opposite carrier by Coulomb interaction and form a bound exciton. The excitons recombine and transfer energy to intra-4f electron of RE^{3+} ions and excite them to high levels. This is one route of energy transfer. The second way is the energy transfer from free electron or hole

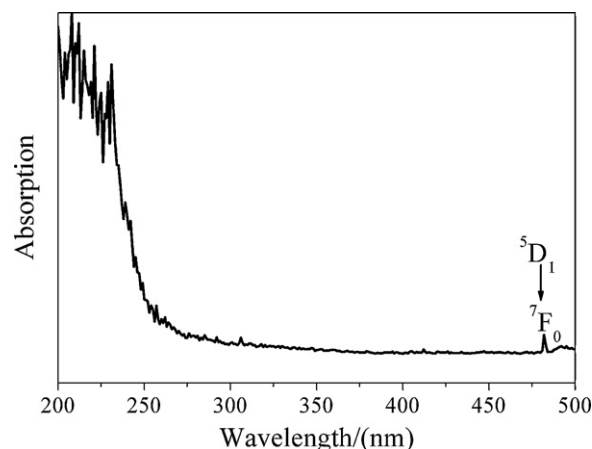


Fig. 5. PLE spectrum for 614 nm emission of Eu^{3+} doped GaN powder.

to the core electrons of RE^{3+} ions by trap occupied by electron or hole [18]. Then RE^{3+} ions can also absorb energy and bound to high levels then generate radiative transition.

4. Conclusions

In summary, GaN:Eu nanoparticles have been synthesized using simple ammonification of Eu-doped Ga_2O_3 powders at different temperatures. Both XRD and TEM patterns appear nano-scale particles with various morphologies. In our analysis, two extra observed GaN Raman shifts with the peaks of 255 and 419 cm^{-1} are attributed to phonon activated by surface disorders and finite-size effects and vibration mode of N-rich octahedral Ga–N₆ bonds, respectively. From PL spectra, five characteristic peaks of Eu^{3+} ions were clearly observed. The synthesized temperature and Eu concentration influence on PL were also studied. Energy transfer process between GaN host and Eu^{3+} ions were also analyzed. All these results mean that nano GaN powder is a very proper host material for REs doping.

References

- [1] S. Shirakata, R. Takashi, K. Sasaki, *Appl. Phys. Lett.* 85 (2004) 2247.
- [2] A.J. Steckl, J.M. Zavada, *MRS Bull.* 24 (1999) 33.
- [3] A.J. Steckl, J.C. Heinkenfeld, D.S. Lee, M.J. Gartner, C.C. Baker, Y. Wong, R. Jones, *IEEE J. Sel. Top. Quantum Electron.* 8 (2002) 749.
- [4] J.H. Kim, N. Shepherd, M.R. Davidson, P.H. Holloway, *Appl. Phys. Lett.* 83 (2003) 641.
- [5] J.H. Kim, N. Shepherd, M.R. Davidson, P.H. Holloway, *Appl. Phys. Lett.* 83 (2003) 4279.
- [6] J.H. Kim, M.R. Davidson, P.H. Holloway, *Appl. Phys. Lett.* 83 (2003) 4746.
- [7] J.H. Kim, P.H. Holloway, *J. Appl. Phys.* 95 (2004) 4787.
- [8] R. Wang, A.J. Steckl, *J. Cryst. Growth* 312 (2010) 680.
- [9] X.J. Pan, Z.X. Zhang, L. Jia, H. Li, E.Q. Xie, *J. Alloys Compd.* 458 (2008) 579.
- [10] A. Podhorodecki, M. Nyk, J. Misiewicz, W. Strek, *J. Lumin.* 126 (2007) 219.
- [11] A. Podhorodecki, M. Nyk, R. Kudrawiec, J. Misiewicz, W. Strek, *Electrochem. Solid State Lett.* 10 (2007) H88.
- [12] E. Brown, U. Hoemmerich, T. Yamada, H. Yamane, J.M. Zavada, *Adv. Mater. Photonic Appl.* 1111 (2009) 97.
- [13] O. Contreras, S. Srinivisan, F.A. Ponce, G.A. Hirata, F. Ramos, J. Mc Kittrick, *Appl. Phys. Lett.* 81 (2002) 1993.
- [14] M. Nyk, R. Kudrawiec, W. Strek, J. Misiewicz, *Opt. Mater.* 28 (2006) 767.
- [15] H. Wu, C.B. Poitras, M. Lipson, M.G. Spencer, J. Hunting, F.J. Di Salvo, *Appl. Phys. Lett.* 88 (2006) 011921.
- [16] L. Jia, E.Q. Xie, X.J. Pan, Z.X. Zhang, Y.Z. Zhang, *Mater. Sci. Technol.* 25 (2009) 1498.
- [17] P. Scherrer, *Göttinger Nachrichten Gesell* 2 (1918) 98.
- [18] W. Gebicki, L. Adamowicz, J. Strzeszewski, S. Podsiadlo, T. Szyszko, G. Kamler, *Mater. Sci. Eng. B* 82 (2001) 182.
- [19] Y.H. Gao, Y. Bando, T. Sato, Y.F. Zhang, X.Q. Gao, *Appl. Phys. Lett.* 81 (2002) 2267.
- [20] J.W. Ortony, C.T. Foxon, *Rep. Prog. Phys.* 61 (1998) 1.
- [21] T. Kanata, H. Murai, K. Kubota, *J. Appl. Phys.* 61 (1987) 969.
- [22] C.C. Chen, C.C. Yeh, C.H. Chen, M.Y. Yu, H.L. Liu, J.J. Wu, *J. Am. Chem. Soc.* 123 (2001) 2791.
- [23] H.L. Liu, C.C. Chen, C.T. Chia, C.C. Yeh, C.H. Chen, M.Y. Yu, *Chem. Phys. Lett.* 345 (2001) 245.

- [24] Z.X. Zhang, X.J. Pan, T. Wang, L. Jia, L.X. Liu, W.B. Wang, E.Q. Xie, J. Electron. Mater. 37 (2008) 1049.
- [25] G.Q. Pan, M.E. Kordesch, P.G. Van Patten, Chem. Mater. 18 (2006) 5392.
- [26] J.Q. Ning, S.J. Xu, D.P. Yu, Y.Y. Shan, S.T. Lee, Appl. Phys. Lett. 91 (2007) 103117.
- [27] E.E. Nyein, U. Hommerich, J. Heikenfeld, D.S. Lee, A.J. Steckl, J.M. Zavada, Appl. Phys. Lett. 82 (2003) 1655.
- [28] L.D. Carlos, A.L.L. Videra, Phys. Rev. B 49 (1994) 11721.
- [29] M. Nyk, J.M. Jablonski, W. Strezk, J. Misiewicz, Opt. Mater. 26 (2004) 133.
- [30] H.J. Lozykowski, Phys. Rev. B 48 (1993) 17758.